

# Determination of bisphosphonates by ion chromatography–inductively coupled plasma mass spectrometry

Miroslav Kovačević<sup>a</sup>, Andrej Gartner<sup>b</sup>, Milko Novič<sup>a,\*</sup>

<sup>a</sup> National Institute of Chemistry, P.O. Box 660, SI-1001 Ljubljana, Slovenia

<sup>b</sup> Krka d.d., Research and Development Division, Šmarješka cesta 6, SI-8501 Novo mesto, Slovenia

Available online 13 February 2004

## Abstract

An ion chromatography–inductively coupled plasma mass spectrometry (IC–ICP–MS) was introduced in the analysis of bisphosphonates. Two compounds (alendronic acid and etidronic acid) were separated on a Dionex AS-7 anion-exchange column with dilute nitric acid employed as the mobile phase. The analytes were detected at  $m/z$  31, as they contain phosphorus. The detection limits achieved were  $0.20 \text{ mg l}^{-1}$  for alendronic acid and  $0.05 \text{ mg l}^{-1}$  for etidronic acid. Since the determination of phosphorus by ICP–MS is difficult due to polyatomic interferences at  $m/z$  31 ( $^{15}\text{N}^{16}\text{O}^+$ ,  $^{14}\text{N}^{16}\text{O}^+\text{H}^+$ , and  $^{12}\text{C}^1\text{H}_3^{16}\text{O}^+$ ), a detailed study of the influence of plasma parameters on phosphorus and background signal was performed.

© 2004 Elsevier B.V. All rights reserved.

**Keywords:** Inductively coupled plasma mass spectrometry; Bisphosphonates; Alendronic acid; Etidronic acid

## 1. Introduction

Bisphosphonates are a class of compounds with characteristic C–PO<sub>3</sub>H<sub>2</sub> groups, which were initially used as complexing agents in water treatment and as detergent additives [1]. Today they are typically used in the treatment of bone diseases, as their ability to bind strongly to the bone matrix inhibits bone resorption [2,3]. Some typical representative compounds from this group are alendronic acid [AMDP, 4-amino-1-hydroxybutane-1,1-bisphosphonic acid, NH<sub>2</sub>–CH<sub>2</sub>–CH<sub>2</sub>–CH<sub>2</sub>–C(PO<sub>3</sub>H<sub>2</sub>)<sub>2</sub>OH] and etidronic acid [HEDP, 1-hydroxyethylidene-1,1-diphosphonic acid, CH<sub>3</sub>–C(PO<sub>3</sub>H<sub>2</sub>)<sub>2</sub>OH]. Bisphosphonates are water-soluble ionic compounds and ion-exchange chromatography, is therefore, the most suitable separation technique. Their ability to chelate metal ions causes analytical problems, since the presence of trace metals in the eluent leads to loss of column performance. A contaminated column retards the bisphosphonates, resulting in severe tailing of the peaks. This retardation is caused by the binding of the bisphosphonates to metals that have been retained by underivatized cation-exchange sites on the anion-exchange

resin, as noted by Daley-Yates et al. [4]. Despite this problem, anion-exchange chromatography is a commonly used separation technique for the separation of bisphosphonates [2,4–11].

Due to the absence of a chromophore in the bisphosphonate molecule, (sensitive) direct spectrophotometric detection after chromatographic separation cannot be applied without appropriate derivatization. In spite of this, bisphosphonates were successfully detected by indirect UV detection [8]. The authors used a UV-absorbing mobile phase (nitric acid) and the decrease of signal at 220 nm was used for quantification of AMDP, with a limit of detection (LOD) of  $1 \text{ mg l}^{-1}$  determined. Indirect conductivity measurements were applied using nitric acid as a mobile phase and an LOD of  $2 \text{ mg l}^{-1}$  was achieved for AMDP [6]. Nitric acid was again used as a mobile phase, and in conjunction with a refractive index detector, an LOD of  $0.4 \text{ mg l}^{-1}$  was obtained for AMDP [7]. When a mobile phase composed of a solution of copper(II) nitrate and nitric acid was employed, bisphosphonate–Cu<sup>2+</sup> complexes were formed and were detected by a UV detector, with a resulting LOD of  $0.4 \text{ mg l}^{-1}$  [9]. An inductively coupled plasma optical emission spectrometer was also used as a detector for bisphosphonates, with a relatively poor LOD of  $\sim 40 \text{ mg l}^{-1}$  achieved for HEDP [10]. Molecular mass spectrometry has seldom been coupled to HPLC for analysis of bisphosphonates,

\* Corresponding author. Tel.: +386-14760200; fax: +386-14760300.  
E-mail address: [milko.novic@ki.si](mailto:milko.novic@ki.si) (M. Novič).

although it has been used for qualitative characterization [11].

Fluorescence detection was applied after postcolumn derivatization of bisphosphonates with a solution of  $\text{Al}^{3+}$ -morin complex, and an LOD of  $0.4 \text{ mg l}^{-1}$  was obtained [1]. When an on-line photochemical reactor with sodium molybdate as a postcolumn derivatization reagent was used, the achieved LOD was  $0.15 \text{ mg l}^{-1}$  [5]. A sensitive, but very complex two-step postcolumn derivatization was developed by Daley-Yates et al. [4]. Bisphosphonates were first oxidized to orthophosphate by ammonium persulphate in a heated reactor coil and molybdenum-ascorbate then added to yield phosphomolybdate, which was detected by absorption at 820 nm, with an LOD of  $10 \text{ } \mu\text{g l}^{-1}$ . A precolumn derivatization method was described by Kline et al. [12,13]. They used 2,3-naphthalene dicarboxaldehyde reagent prior to reverse phased HPLC with fluorescence detection. Limits of quantification in the range  $1\text{--}5 \text{ } \mu\text{g l}^{-1}$  in urine and plasma samples were achieved.

As phosphorus is present in bisphosphonates, inductively coupled plasma mass spectrometry (ICP-MS) can be used as an element-specific detection method. However, determination of phosphorus by ICP-MS at trace levels is difficult due to the high ionization potential of phosphorus and consequently its low ionization efficiency in an argon plasma. It also suffers from polyatomic interferences at  $m/z$  31, when a quadrupole (low mass resolution) instrument is used. Hence not only  $^{31}\text{P}^+$  ions, but also polyatomic ions such as  $^{15}\text{N}^{16}\text{O}^+$ ,  $^{14}\text{N}^{16}\text{O}^1\text{H}^+$ , and  $^{12}\text{C}^1\text{H}_3^{16}\text{O}^+$  are measured [14,15]. The formation of these ions in plasma is unavoidable, due to the presence of the elements carbon, nitrogen, and oxygen in samples, in plasma gas and in the laboratory environment. As a result, higher limits of detection are achieved if these elements are present in the mobile phase. Despite the described limitations, many authors have reported the successful use of a quadrupole ICP-MS system (without collision/reaction cell technology) as a detector for liquid chromatography of phosphorus compounds. An orthophosphate and some condensed phosphates were analyzed with detection limits from 8 to  $20 \text{ } \mu\text{g l}^{-1}$  of phosphorus [16–18], while detection limits from 16 to  $80 \text{ } \mu\text{g l}^{-1}$  of phosphorus were determined upon analysis of adenosine phosphates [16].

Considering the sensitive detection of different phosphorus compounds as mentioned above, we were prompted to introduce a quadrupole ICP-MS system as a detector for bisphosphonates, following the ion-exchange chromatography procedure reported by Daley-Yates et al. [4], due to the current demand for sensitive but uncomplicated detection techniques. A detailed study of the influence of plasma parameters, using dilute nitric acid as a mobile phase, on system performance is given. In addition, the detector capabilities in the case of two model compounds (AMDP and HEDP) are shown.

## 2. Experimental

### 2.1. Reagents

Deionized water ( $18 \text{ M}\Omega \text{ cm}$ ) used in this study was prepared using a Milli-Q system (Millipore, Bedford, MA, USA). Nitric acid (analytical-reagent grade, 65%, Merck, Darmstadt, Germany),  $\text{KH}_2\text{PO}_4$  (analytical-reagent grade, min. 99.5%, Merck), etidronic acid (Fluka, Buchs, Switzerland) and monosodium alendronate trihydrate (Krka, Novo mesto, Slovenia) were used for preparation of the carrier solution, mobile phase, and standard solutions.

### 2.2. Chromatography and flow injection system

An inert quaternary pump Spectra System P4000 (Thermo Separation Products, Mountain View, CA, USA), inert manual injector ( $50 \text{ } \mu\text{l}$ ) (Rheodyne, Cotati, CA, USA) and AS7 ( $4 \times 250 \text{ mm}$ ) analytical column with AG7 ( $4 \times 50 \text{ mm}$ ) guard column (Dionex, Sunnyvale, CA, USA) were used for separation. A metal trap column MFC-1 (Dionex) was installed between the pump and injector. For measurements of AMDP and HEDP, mobile phases containing  $1.5 \text{ mmol l}^{-1}$  nitric acid ( $1.4 \text{ ml min}^{-1}$ ) and  $15 \text{ mmol l}^{-1}$  nitric acid ( $1.0 \text{ ml min}^{-1}$ ) were used, respectively. The configuration of the flow injection analysis (FIA) system was the same as that of the chromatography system, with the exception that the columns were replaced by an appropriate back-pressure coil that maintained the back-pressure at  $1000 \text{ p.s.i.}$  at a flow rate  $1.0 \text{ ml min}^{-1}$  ( $1 \text{ p.s.i.} = 6894.76 \text{ Pa}$ ).

### 2.3. ICP-MS detection

Coupling of the ion chromatography (IC) and FIA systems to ICP-MS was performed through connection of the exit from the column (and from the FIA system) to the Babington type nebulizer of the ICP-MS HP4500plus instrument (Agilent, Waldbronn, Germany). The following plasma conditions were applied for detection of bisphosphonates: plasma gas flow rate,  $15.01 \text{ min}^{-1}$ ; auxiliary gas flow rate,  $0.901 \text{ min}^{-1}$ ; carrier gas flow rate,  $1.081 \text{ min}^{-1}$ ; radio frequency (RF) power,  $1600 \text{ W}$ ; spray chamber temperature,  $2 \text{ }^\circ\text{C}$ ; sampling depth (torch-interface distance),  $7 \text{ mm}$ ; signal sampling time,  $0.3 \text{ s}$ .

## 3. Results and discussion

### 3.1. Optimization of detector response

The initial instrument tuning was based on direct introduction of a solution containing  $10 \text{ } \mu\text{g l}^{-1}$  each of the elements lithium, yttrium, cerium and thallium in 2% nitric acid using a peristaltic pump ( $0.30 \text{ ml min}^{-1}$ ). The instrument was optimized for high sensitivity towards these elements and simultaneously for minimum cerium oxide ratio

(ratio between abundance of  $\text{Ce}^+$  and  $\text{CeO}^+$  ions in plasma, which is the measure for efficient sample decomposition) by adjusting the RF power to 1300 W, the carrier gas flow rate to  $1.05 \text{ l min}^{-1}$  and the sampling depth to 6 mm. In addition, the mass analyzer parameters were adjusted to achieve good mass separation between the mass peak at  $m/z$  31 and the neighboring peaks. The goal of further optimization of the detector response was to find suitable plasma parameters to provide high sensitivity towards phosphorus, as well as a low background signal (lowest abundance of polyatomic ions). Due to higher flexibility and a faster response time required for system optimization, the FIA system was used for optimization of detector parameters. The carrier solution was  $20 \text{ mmol l}^{-1}$  nitric acid and the sample was a  $1.6 \text{ mg l}^{-1}$  solution of HEDP in  $20 \text{ mmol l}^{-1}$  nitric acid, which was pumped at a flow rate of  $1.0 \text{ ml min}^{-1}$ . The height of the transient FIA signal was considered as the phosphorus signal and the height of baseline of the FIA signal as the background signal. The ratio between the phosphorus signal and the background signal (SB ratio) was used as the criterion for evaluation of detector performance.

The first step of plasma conditions optimization was to find the appropriate RF power (Fig. 1). Since conditions within the plasma change with the distance from the plasma source to the sampling point (sampling depth), optimization was conducted at three different sampling depths (5, 7, and 9 mm). The highest SB ratio was always obtained at the highest RF power (1600 W), since higher temperatures are required for improved ionization of phosphorus and for decomposition of polyatomic ions. However, the dependence on RF power varies at different sampling depths. When sampling at a distance of 5 mm, SB ratios were poor, due to the shorter residence times of sample in the plasma. Only at higher power was there sufficient energy for high SB ratios. On the contrary, sampling at 9 mm gave relatively constant SB ratios at applied powers higher than 1200 W, which means that the residence time is long enough for decomposi-

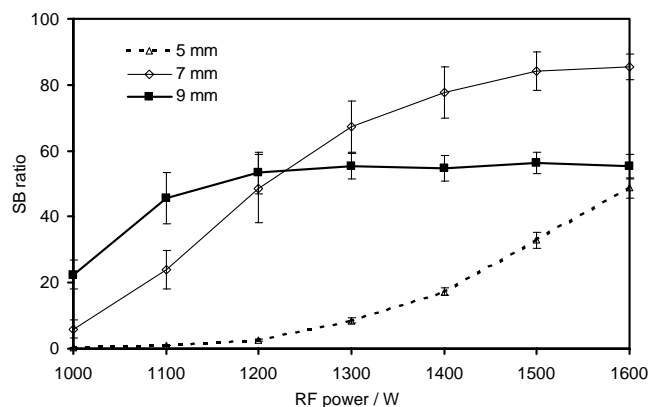


Fig. 1. Influence of RF power on signal-to-background ratio at sampling depths of 5, 7, and 9 mm (error bars represent  $\pm 1$  S.D.). Experimental conditions: carrier solution,  $20 \text{ mmol l}^{-1}$   $\text{HNO}_3$ ; flow rate,  $1.0 \text{ ml min}^{-1}$ ; sample,  $1.6 \text{ mg l}^{-1}$  HEDP in  $20 \text{ mmol l}^{-1}$   $\text{HNO}_3$ ; sample volume,  $50 \mu\text{l}$ ; carrier gas flow rate,  $1.05 \text{ l min}^{-1}$ .

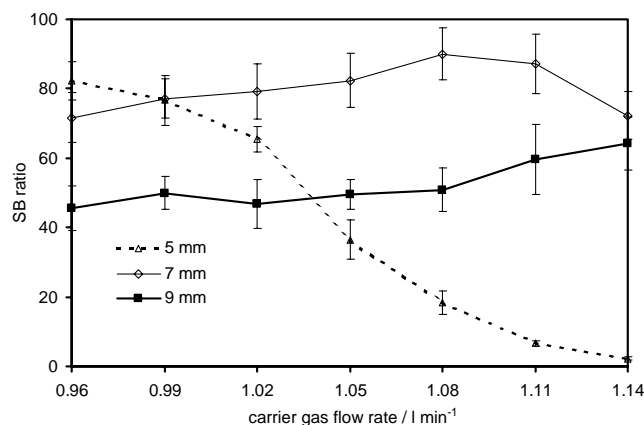


Fig. 2. Influence of carrier gas flow rate on signal-to-background ratio at sampling depths of 5, 7, and 9 mm (error bars represent  $\pm 1$  S.D.). Experimental conditions: carrier solution,  $20 \text{ mmol l}^{-1}$   $\text{HNO}_3$ ; flow rate,  $1.0 \text{ ml min}^{-1}$ ; sample,  $1.6 \text{ mg l}^{-1}$  HEDP in  $20 \text{ mmol l}^{-1}$   $\text{HNO}_3$ ; sample volume,  $50 \mu\text{l}$ ; RF power 1600 W.

tion of the sample. However, SB ratios were lower than those obtained with a sampling point of 7 mm, which is probably close to optimum. Accordingly, an RF power of 1600 W was chosen for further optimization and routine measurements.

The next step in plasma optimization was the study of the effects of different carrier gas flow rates in the range  $0.96\text{--}1.14 \text{ l min}^{-1}$  at RF power 1600 W (Fig. 2). Since different carrier gas flow rates shift the optimum point of sampling due to changes in velocity in the central channel of the plasma, the complete experiment was conducted at three different sampling depths. The highest SB ratio was found at a flow rate of  $1.08 \text{ l min}^{-1}$ , when the sampling point was 7 mm from the torch. Therefore, these conditions were chosen for the next step of the optimization procedure and for further experiments. When the sampling point was located closer to the torch (5 mm), the optimal carrier gas flow rate was lower ( $0.96 \text{ l min}^{-1}$ ), while sampling the plasma at a longer distance (9 mm), resulted in a higher optimal carrier gas flow rate ( $1.14 \text{ l min}^{-1}$ ).

To find the optimal sampling depth at RF power 1600 W and carrier gas flow rate  $1.08 \text{ l min}^{-1}$ , depths from 4 to 11 mm were tested (Fig. 3). The phosphorus signal decreases with the increased sampling depth, since the density of ions in the central channel of the plasma decreases. Concerning the phosphorus signal alone, the smallest depth would be optimal. However, the background signal is extremely high at depths of 4 mm ( $\sim 40\,000$  counts—out of range in Fig. 3a), and it rapidly decreases when approaching distances of 6–7 mm. It reaches its minimal value at distances between 8 and 9 mm. This is as expected, since a longer torch-interface distance means a longer residence time in the plasma, and hence more decomposition of polyatomic ions. However, at distances longer than 10 mm, the background starts to increase again, probably due to lower temperatures in the plasma, and due to diffusion of air from the atmosphere into the plasma. Calculated SB ratios (Fig. 3b) show

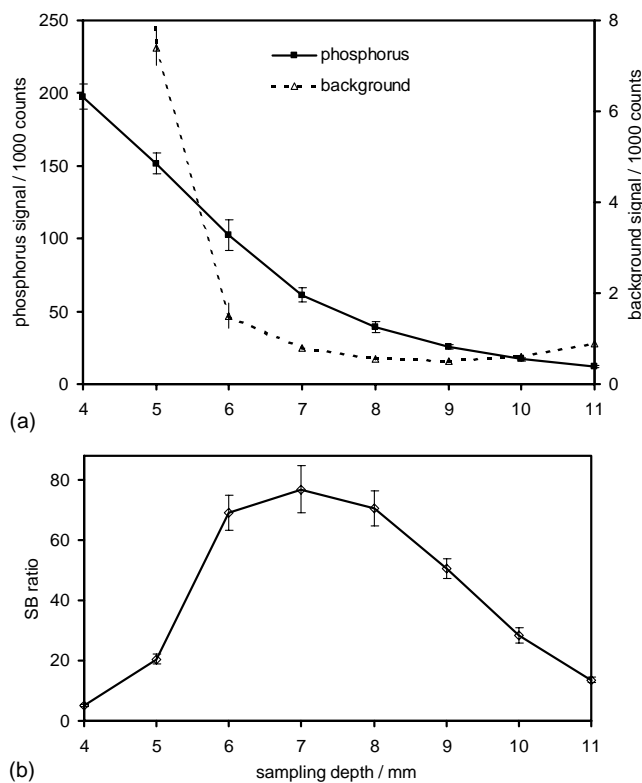


Fig. 3. Influence of sampling depth on phosphorus and background signal (a) and on signal-to-background ratio (b) (error bars represent  $\pm 1$  S.D.). Experimental conditions: carrier solution,  $20 \text{ mmol l}^{-1} \text{ HNO}_3$ ; flow rate,  $1.0 \text{ ml min}^{-1}$ ; sample,  $1.6 \text{ mg l}^{-1}$  HEDP in  $20 \text{ mmol l}^{-1} \text{ HNO}_3$ ; sample volume,  $50 \mu\text{l}$ ; RF power  $1600 \text{ W}$ ; carrier gas flow rate  $1.081 \text{ min}^{-1}$ .

that the highest ratio between phosphorus and background signal is at a torch-interface distance of 7 mm. Therefore, for routine measurements, a distance of 7 mm was chosen.

### 3.2. Influence of mobile phase composition and flow rate on detector response

To investigate the influence of nitric acid concentration in the mobile phase on detector performance, a FIA signal of HEDP solution was recorded in the concentration range of nitric acid usually applied for separation of bisphosphonates ( $0\text{--}50 \text{ mmol l}^{-1}$ ) at a flow rate of  $1.0 \text{ ml min}^{-1}$  (Fig. 4). It was found that the phosphorus signal was practically the identical throughout the whole concentration range of nitric acid. At the same time, the background signal increased proportionally with increasing nitric acid concentration. The sources of background signal at zero concentration (deionized water) are probably impurities in the argon gas and air from the laboratory environment. The values measured for background signal changed from 410 counts at zero concentration to 770 counts at a concentration of  $50 \text{ mmol l}^{-1}$ . This increase was as expected, since nitric acid is a source of nitrogen, which forms nitrogen-based polyatomic ions in plasma. This effect has significance in optimization of the chromatographic separation, since the concentration of ni-

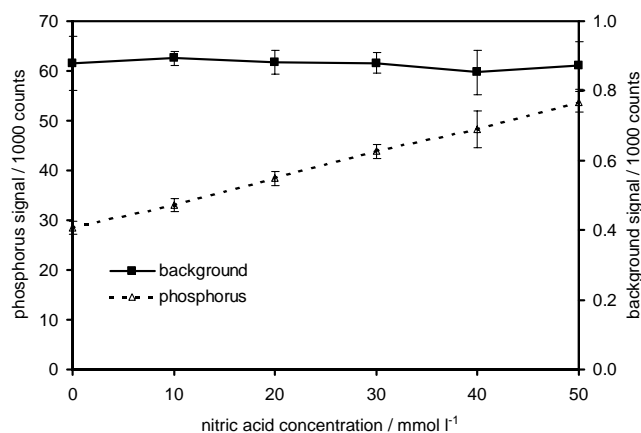


Fig. 4. Influence of nitric acid concentration in carrier solution on phosphorus and background signals (error bars represent  $\pm 1$  S.D.). Experimental conditions: flow rate,  $1.0 \text{ ml min}^{-1}$ ; sample,  $1.6 \text{ mg l}^{-1}$  HEDP in carrier solution; sample volume,  $50 \mu\text{l}$ ; RF power  $1600 \text{ W}$ ; carrier gas flow rate  $1.081 \text{ min}^{-1}$ ; sampling depth, 7 mm.

tric acid is an important factor for adjustment of retention times. As a consequence, higher concentrations of nitric acid in the mobile phase will increase the baseline signal and poorer detection limits will be achieved.

Another important parameter for chromatographic separation is the mobile phase flow rate. Throughout all experiments devoted to detector optimization, the height of the FIA signal and the height of the background signal were considered. However, the carrier solution flow rate influences the shape of the FIA signal because the residence time of an analyte in the detector changes. To avoid this effect, the area of the phosphorus peak was considered as the phosphorus signal. To evaluate background, its area from the starting point to the beginning of the phosphorus signal was measured and considered as a measure for background intensity. The results are given in Fig. 5. An increase of background

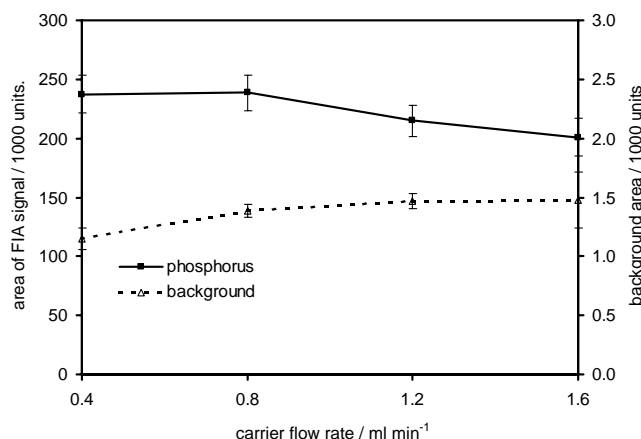


Fig. 5. Influence of flow rate of carrier solution on phosphorus and background signals (error bars represent  $\pm 1$  S.D.). Experimental conditions: carrier solution,  $20 \text{ mmol l}^{-1} \text{ HNO}_3$ ; sample,  $1.6 \text{ mg l}^{-1}$  HEDP in  $20 \text{ mmol l}^{-1} \text{ HNO}_3$ ; sample volume,  $50 \mu\text{l}$ ; RF power  $1600 \text{ W}$ ; carrier gas flow rate  $1.081 \text{ min}^{-1}$ ; sampling depth, 7 mm.

and decrease of phosphorus signal was noted. A higher flow rate means more solvent in the plasma, which causes cooling of the central channel of the plasma. Therefore, lower temperatures are the reason for less efficient ionization of phosphorus and less efficient decomposition of polyatomic ions.

### 3.3. Chromatographic separation and quantification

In the study of the influence of mobile phase composition and flow rate on the detector response, it was shown that higher concentrations of nitric acid and higher mobile phase flow rates have a negative effect on the sensitive detection of phosphorus (Section 3.2). However, it was assumed that these effects do not influence the limits of detection significantly; and therefore, the chromatographic conditions described in the literature were applied for demonstration of detector capabilities [4]. As a possible inorganic contaminant, orthophosphate was also included in the study. The “reference” chromatographic conditions [4] were modified by applying  $1.5 \text{ mmol l}^{-1}$  nitric acid as a mobile phase with a flow rate of  $1.4 \text{ ml min}^{-1}$  (Fig. 6). The retention times for AMDP and orthophosphate were 5.5 min ( $k' = 3.2$ ) and 10.1 min ( $k' = 6.8$ ), respectively. The total chromatographic run-time was 14 min. The application of a relatively long run-time was necessary due to tailing of the AMDP peak. The optimal separation of orthophosphate and HEDP was achieved at flow rate of  $1.0 \text{ ml min}^{-1}$  with  $15 \text{ mmol l}^{-1}$  nitric acid as the mobile phase (Fig. 7). The retention times for HEDP and orthophosphate were 3.6 min ( $k' = 1.3$ ) and 1.9 min ( $k' = 0.2$ ), respectively. The total chromatographic run-time was 8 min.

The linearity coefficient for AMDP determination was 0.9998, within the concentration range  $0.6\text{--}20 \text{ mg l}^{-1}$ . The linear concentration range was limited at higher concentrations due to the co-elution of orthophosphate with the tailing AMDP peak. The detection limit, determined as three

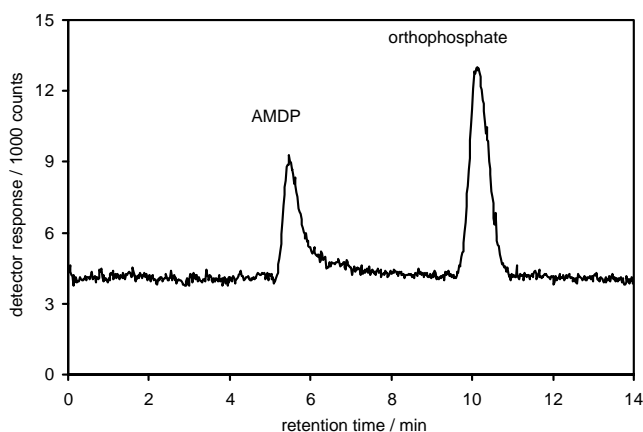


Fig. 6. Separation of AMDP and orthophosphate. Experimental conditions: mobile phase,  $1.5 \text{ mmol l}^{-1}$   $\text{HNO}_3$ ,  $1.4 \text{ ml min}^{-1}$ ; sample,  $1 \text{ mg l}^{-1}$  AMDP and  $0.77 \text{ mg l}^{-1}$  orthophosphate; sample volume,  $50 \mu\text{l}$ ; RF power  $1600 \text{ W}$ ; carrier gas flow rate  $1.081 \text{ min}^{-1}$ ; sampling depth,  $7 \text{ mm}$ .

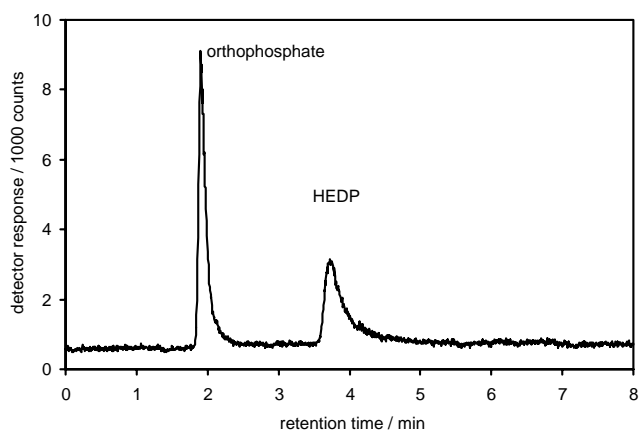


Fig. 7. Separation of HEDP and orthophosphate ( $0.77 \text{ mg l}^{-1}$ ). Experimental conditions: mobile phase,  $15 \text{ mmol l}^{-1}$   $\text{HNO}_3$ ,  $1.0 \text{ ml min}^{-1}$ ; sample,  $0.83 \text{ mg l}^{-1}$  HEDP and  $0.77 \text{ mg l}^{-1}$  orthophosphate; sample volume,  $50 \mu\text{l}$ ; RF power  $1600 \text{ W}$ ; carrier gas flow rate  $1.081 \text{ min}^{-1}$ ; sampling depth,  $7 \text{ mm}$ .

times the baseline noise, was  $0.20 \text{ mg l}^{-1}$ . The reproducibility was  $\pm 8\%$  at  $1 \text{ mg l}^{-1}$ . The linear range for HEDP was from  $0.16$  to  $16 \text{ mg l}^{-1}$ , with a linearity coefficient of 0.9999. The detection limit, again estimated as three times the baseline noise, was  $0.05 \text{ mg l}^{-1}$ . The reproducibility determined for all concentration points was in the range from  $\pm 4$  to  $\pm 6\%$ .

## 4. Conclusions

An ICP-MS system can be used for sensitive detection of phosphorus compounds despite the existence of polyatomic interferences, which can be minimized by optimization of conditions in the plasma. In addition, it is shown that dilute nitric acid used as a mobile phase does not contribute significantly to the height of the chromatogram baseline at the applied concentrations, and that the main sources of background signal are impurities in the plasma gas and/or in the air surrounding the plasma. The influence of the mobile phase flow rate on detector response can also be neglected. Upon comparison with other detection techniques, the quadrupole ICP-MS enables simple and more sensitive detection of bisphosphonates. However, it does not achieve as low detection limits as those obtained with rather complex pre and postcolumn derivatization methods [4,12,13]. The drawback of the introduced method is relatively poor reproducibility due to peak tailing, which could be attributed to the polyprotic nature of bisphosphonates indicated in the data on acid constants (HEDP:  $\text{p}K_1 = 1.35$ ;  $\text{p}K_2 = 2.87$ ;  $\text{p}K_3 = 7.03$  in  $\text{p}K_4 = 11.3$  and AMDP:  $\text{p}K_1 = 2.72$ ;  $\text{p}K_2 = 8.73$ ;  $\text{p}K_3 = 10.5$  in  $\text{p}K_4 = 11.6$ ) [19]. The detection limits and reproducibility could be improved by minimizing peak tailing through addition of modifiers to the mobile phase. However, detection of phosphorus at  $m/z$  31 by a quadrupole ICP-MS is subject to polyatomic interferences



derived from carbon containing compounds ( $^{31}\text{CH}_3\text{O}^+$ ). According to literature data [15], their presence would result in increased background, thus addition of any carbon compounds to the mobile phase was avoided.

### Acknowledgements

The authors thank the Ministry of Education, Science and Sport of the Republic of Slovenia for financial support (contract nos. S16-416-004/19054/98 and P1-0509-0104).

### References

- [1] M.J. Lovdahl, D.J. Pietrzyk, J. Chromatogr. A 850 (1999) 143.
- [2] R.W. Sparidans, J. den Hartigh, Pharm. World Sci. 21 (1999) 1.
- [3] J.H. Lin, Bone 18 (1996) 75.
- [4] P.T. Daley-Yates, L.A. Gifford, C.R. Hoggarth, J. Chromatogr. 490 (1989) 329.
- [5] S.X. Peng, S.M. Dansereau, J. Chromatogr. A 914 (2001) 105.
- [6] E.W. Tsai, D.P. Ip, M.A. Brooks, J. Chromatogr. 596 (1992) 217.
- [7] Y.R. Han, X. Qin, J. Chromatogr. A 719 (1996) 345.
- [8] E.W. Tsai, S.D. Chamberlin, R.J. Forsyth, C. Bell, D.P. Ip, M.A. Brooks, J. Pharm. Biomed. Anal. 12 (1994) 983.
- [9] R.W. Sparidans, J. den Hartigh, P. Vermeij, J. Pharm. Biomed. Anal. 13 (1995) 1545.
- [10] K.A. Forbes, J. Vecchiarelli, P.C. Uden, R.M. Barnes, in: P. Jandik, R.M. Cassidy (Eds.), Advances in Ion Chromatography, Proceedings of the International Ion Chromatography Forum, Century International, Franklin, MA, 1989, p. 487.
- [11] X. Qin, E.W. Tsai, T. Sakuma, D.P. Ip, J. Chromatogr. A 686 (1994) 205.
- [12] W.F. Kline, B.K. Matuszewski, W.F. Bayne, J. Chromatogr. 534 (1990) 139.
- [13] W.F. Kline, B.K. Matuszewski, J. Chromatogr. 583 (1992) 183.
- [14] H. Wildner, J. Anal. At. Spectrom. 13 (1998) 573.
- [15] M. Wind, M. Edler, N. Jakubowski, M. Linscheid, H. Wesch, W.D. Lehmann, Anal. Chem. 73 (2001) 29.
- [16] S. Jiang, R.S. Houk, Spectrochim. Acta B43 (1988) 405.
- [17] R.G. Fernandez, J.I.G. Alonso, A. Sanz-Medel, J. Anal. At. Spectrom. 16 (2001) 1035.
- [18] B. Divjak, M. Novič, W. Goessler, J. Chromatogr. A 862 (1999) 39.
- [19] M.J. O'Neil (Ed.), The Merck Index, Merck & Co., Whitehouse Station, NJ, 2001.